

NBSIR 73-268

Laser Damage in Materials

Albert Feldman, Deane Horowitz, and Roy M. Waxler

Solid State Materials Section
Inorganic Materials Division
Institute for Materials Research
National Bureau of Standards
Washington, D. C. 20234

August 1973

Semi-Annual Technical Report
Period Covered: February 1, 1973, to July 31, 1973

Prepared for
Advanced Research Projects Agency
Arlington, Virginia 22209

ARPA Order No. 2016

NBSIR 73-268

LASER DAMAGE IN MATERIALS

Albert Feldman, Deane Horowitz, and Roy M. Waxler

Solid State Materials Section
Inorganic Materials Division
Institute for Materials Research
National Bureau of Standards
Washington, D. C. 20234

August 1973

Semi-Annual Technical Report
Period Covered: February 1, 1973, to July 31, 1973

Prepared for
Advanced Research Projects Agency
Arlington, Virginia 22209
ARPA Order No. 2016



U. S. DEPARTMENT OF COMMERCE, Frederick B. Dent, Secretary
NATIONAL BUREAU OF STANDARDS, Richard W. Roberts, Director

LASER DAMAGE IN MATERIALS

Albert Feldman, Deane Horowitz, and Roy M. Waxler

Solid State Materials Section
Inorganic Materials Division
Institute for Materials Research

ARPA Order No.	2016
Program Code Number.	3D10
Effective Date of Contract	January 1, 1972
Contract Expiration Date	December 31, 1973
Principal Investigator	Albert Feldman (301) 921-2840

This is a progress report. The work is incomplete and is continuing. The views and conclusions contained in this document are those of the authors and should not be interpreted as necessarily representing the official policies, either expressed or implied, of the Advanced Research Projects Agency or the U. S. Government.

LASER DAMAGE IN MATERIALS

Abstract

Neodymium:glass laser induced damage is observed in lithium niobate (LiNbO_3), calcite (CaCO_3), potassium dihydrogen phosphate (KDP), and deuterated potassium dihydrogen phosphate (KD^*P). The damage at the lowest power levels is caused by inclusions. At higher power levels, filamentary damage, which is indicative of self-focusing, is observed in LiNbO_3 . An analysis of self-focusing data in yttrium aluminum garnet (YAG) shows that the Kerr effect is the dominant self-focusing mechanism, with some contribution from the thermal effect. Bulk and surface damage thresholds in neodymium-doped thoria:yttrium oxide ceramic are obtained relative to bulk damage thresholds in several optical materials. For solid materials, relationships are obtained between the stress-optic coefficients and the electrostrictive coefficients under different geometric boundary conditions.

Table of Contents

1. Technical Report Summary	1
1.1 Technical Problem.	1
1.2 General Methodology.	2
1.3 Technical Results.	2
1.4 Department of Defense Implications	3
1.5 Implications for Further Research.	4
2. Technical Report	5
2.1 Damage Studies in Lithium Niobate (LiNbO_3), Calcite (CaCO_3), Potassium Dihydrogen Phosphate (KDP), and Deuterated Potassium Dihydrogen Phosphate (KD*P) .	5
2.1.1 Introduction	5
2.1.2 Experimental Procedure	7
2.1.3 Results and Discussion	7
2.2 Self-Focusing in Yttrium Aluminum Garnet	20
2.3 Damage in a Neodymium-Doped Thoria:Yttrium Oxide Ceramic Laser Rod.	23
2.4 Relations Between Electrostriction and the Stress- Optic Effect	27
2.4.1 Case I	31
2.4.2 Case II.	33
2.4.3 Case III	34
2.5 Acknowledgments.	35
2.6 References	37

LASER DAMAGE IN MATERIALS

1. Technical Report Summary

1.1 Technical Problem

The main objective of this program is the measurement of damage thresholds and the determination of mechanisms associated with self-focusing in materials used in high-energy pulsed laser systems. Self-focusing is the main process which leads to intrinsic bulk damage in laser materials. The damage appears as filamentary tracks in materials exposed to high-intensity laser radiation. The study of self-focusing can be obscured, however, if extrinsic damage processes, such as inclusion damage, take place.

In this report we examine the bulk damage processes in crystalline materials, some of which are used in the fabrication of modulators and Q-switches. We attempt to determine whether inclusions or self-focusing induced damage are the limiting damage factors in these materials. When self-focusing is important, we estimate the relative importance of three mechanisms responsible for self-focusing; the Kerr, electrostrictive, and thermal effects. Additionally, in a theoretical analysis we attempt to resolve an apparent discrepancy between different authors in relations between the electrostrictive coefficients and the stress-optic coefficients.

1.2. General Methodology

Laboratory experiments were conducted to determine the mechanisms of damage in calcite (CaCO_3), potassium dihydrogen phosphate (KDP), deuterated potassium dihydrogen phosphate (KD^*P), lithium niobate (LiNbO_3), and neodymium-doped thoria:yttrium oxide ceramic. The output of a Q-switched Nd:glass laser operating in the TEM_{00} mode was focused into the samples with a 181-mm focal length lens. Damage sites in the samples were examined to ascertain whether inclusion damage or self-focusing induced damage were the limiting damage processes. In undoped yttrium aluminum garnet (YAG), for which earlier measurements indicated self-focusing damage was present, we calculated a lower bound to the nonlinear index n_2 and the individual contributions of the Kerr effect, electrostriction, and the thermal effect to n_2 . We have derived relationships between the electrostrictive coefficients and the stress-optic coefficients for different geometric boundary conditions using thermodynamic arguments in order to resolve an apparent discrepancy in the results of different authors. Thermodynamic free energy relationships were constructed and sets of Maxwell's equations were obtained by taking appropriate derivatives of the free energy.

1.3. Technical Results

We find in calcite, KDP, KD^*P , and LiNbO_3 that inclusions are the limiting cause of damage (section 2.1). In LiNbO_3 we also find evidence for self-focusing, but this occurs at higher power levels.

We analyze previously reported self-focusing data in YAG (section 2.2) which was obtained with both linearly and circularly

polarized radiation. We find that the Kerr effect is the dominant self-focusing mechanism, with some contribution from the thermal effect. The electrostrictive effect is negligible because YAG has exceedingly small stress-optic coefficients. Using the theory which we developed in our previous report, we calculate a lower bound to the nonlinear index n_2 and the contributions of the Kerr and thermal effects to n_2 .

Bulk damage measurements were made in a neodymium-doped thoria:yttrium oxide ceramic laser rod (section 2.3) in cooperation with Charles Greskovich of the General Electric Corporate Research and Development Laboratory*. The damage threshold relative to several optical materials was tabulated.

We have obtained relationships between the stress-optic coefficients and the electrostriction coefficients for three geometric situations (2.4). Our derivation is based on earlier theoretical work. We find that the differing results of several authors correspond to solutions for different geometric boundary conditions.

1.4. Department of Defense Implications

The Department of Defense has a need for high-powered solid state laser systems. Thus it is important (1) to understand the processes which limit the output power of such systems, (2) to obtain data which suggest methods for increasing the output power of a given system, and (3) to verify theories which predict the performance of such systems.

*Research sponsored by ARPA.

We have come to the following conclusions: (1) In materials for which self-focusing is the dominant mechanism leading to damage, such as glasses, sapphire, and YAG, the Kerr effect is the dominant self-focusing mechanism. The Kerr effect increases with increasing refractive index; therefore, for this type of materials, those having low refractive indices will have high self-focusing thresholds. (2) The thermal effect can be important for pulse widths ≥ 25 ns or for high repetition rate systems. (3) Inclusion damage limits the performance of many crystals used presently in modulators and Q-switches, such as calcite, KDP, KD*P, and LiNbO_3 . In order to obtain higher damage thresholds, methods must be found to eliminate the inclusions. When this is done, self-focusing will then become the limiting process.

1.5. Implications for Further Research

For the remainder of the contract period we intend to study two problems. (1) We plan to examine in some detail the process of damage in several neodymium-doped laser glasses, which we discussed in our previous report, in order to determine the self-focusing mechanisms in these materials. (2) We plan to examine the self-focusing computer solutions of Dawes and Marburger so that we can better relate our damage data to the nonlinear index n_2 .

The interests of the Department of Defense have been shifting to longer wavelengths in the infrared ($10.6 \mu\text{m}$ for the CO_2 laser and $3.8 \mu\text{m}$ for the DF laser). Interest is also expected to shift toward the ultraviolet region even though there are still no important high-power lasers in this region. Over this wide wavelength range there is

a lack of data on optical materials that could be used for the construction of optical components. These data include changes of refractive index with temperature and stress which are important because components subjected to high-intensity radiation can undergo a significant change of refractive index due to heat generated by low-level absorption processes. These changes in index are caused by variations of temperature and by stresses introduced by temperature gradients. Therefore, measurements of the refractive index and the change of refractive index with temperature and stress, in both the infrared and ultraviolet regions of the spectrum, would be worthwhile. Materials of current interest in the infrared region are KCl, ZnSe, sapphire, and the alkaline-earth fluorides.

2. Technical Report

2.1. Damage Studies in Lithium Niobate (LiNbO_3), Calcite (CaCO_3), Potassium Dihydrogen Phosphate (KDP), and Deuterated Potassium Dihydrogen Phosphate (KD^*P)

2.1.1. Introduction

The output of high-powered laser systems is limited by the damage occurring in components exposed to the intense electromagnetic radiation. Modulators and Q-switches are important components of pulsed solid-state laser systems. Polarizers and Pockels cells are key elements in many of these components. Polarizers are constructed from prisms of calcite or from glass plates stacked at the Brewster angle. Pockels cells are fabricated from electro-optic crystals; the most common materials are KDP, KD^*P , and LiNbO_3 .

Several authors have published results of damage studies in these materials. Poplavskii and Khazov have reported observing polarization dependent bulk damage in calcite crystals [1]. They were of the opinion that self-focusing was definitely important in calcite although they had not observed filamentary tracks typical of self-focusing induced damage.

Damage studies in KDP and LiNbO_3 have shown that inclusion damage is the limiting process [2,3]. Hence, most damage studies in KDP and LiNbO_3 have emphasized surface damage [4-8] and the statistical nature of this damage process [7,8]. Bass [9] has also examined filamentary damage in LiNbO_3 and has discussed the possibility that self-focusing due to heating is important in producing the damage.

In this report we attempt to identify the principal mechanisms responsible for bulk damage in optical quality calcite, KDP, KD^*P , and LiNbO_3 . We are motivated by the success we have had in identifying the mechanisms responsible for self-focusing induced damage in several optical glasses [10-12]. The conclusion we reach is that inclusions are the principal cause of damage in the above crystals although filamentary damage caused by self-focusing is observed in LiNbO_3 . Recent work by Norman Boling [13] shows that inclusions can be a major factor in surface damage.

2.1.2. Experimental Procedure

The output of a Q-switched Nd:glass laser is focused into the samples with a 181-mm focal length lens. The characterization of the experimental apparatus and the laser beam is discussed in a previous report [10] and is summarized as follows. The laser operates in the TEM₀₀ mode with a pulse width of 25 ns. The pulse energy is constant to within $\pm 2\%$. The focusing lens is located approximately five meters from the spatial mode selection aperture in the oscillator cavity. The beam profile at the position of the focusing lens approximates a Gaussian distribution.

The procedure followed was to fire the laser into the sample and to observe whether damage was produced. If internal damage occurred, the sample was moved laterally to the beam and another laser pulse, of lower energy, was fired into the sample. The laser energy was lowered by inserting a calibrated neutral-density filter into the beam. If damage did not occur, the laser energy was raised. In all cases damage was observed when no filters were present in the beam. When several damage sites were produced with a single laser pulse, they appeared to be co-linear.

2.1.3. Results and Discussion

Figures 1 to 3 show the damage produced in calcite. The calcite is of schlieren grade material. Figure 1 shows the damage in transmitted white light; figure 2 shows the damage with side-light illumination. Both photographs were taken through a polarizer to



Fig. 1. Damage sites in calcite as observed in linearly polarized transmitted white light. The vertical lines define the planes of focus, the left for the ordinary ray and the right for the extraordinary ray. The arrow to the right shows the direction of laser beam propagation, which was perpendicular to the optic axis. Sites whose ordinates are above the arrow were produced with the extraordinary ray, those below the arrow with ordinary ray. The magnification is 9X.

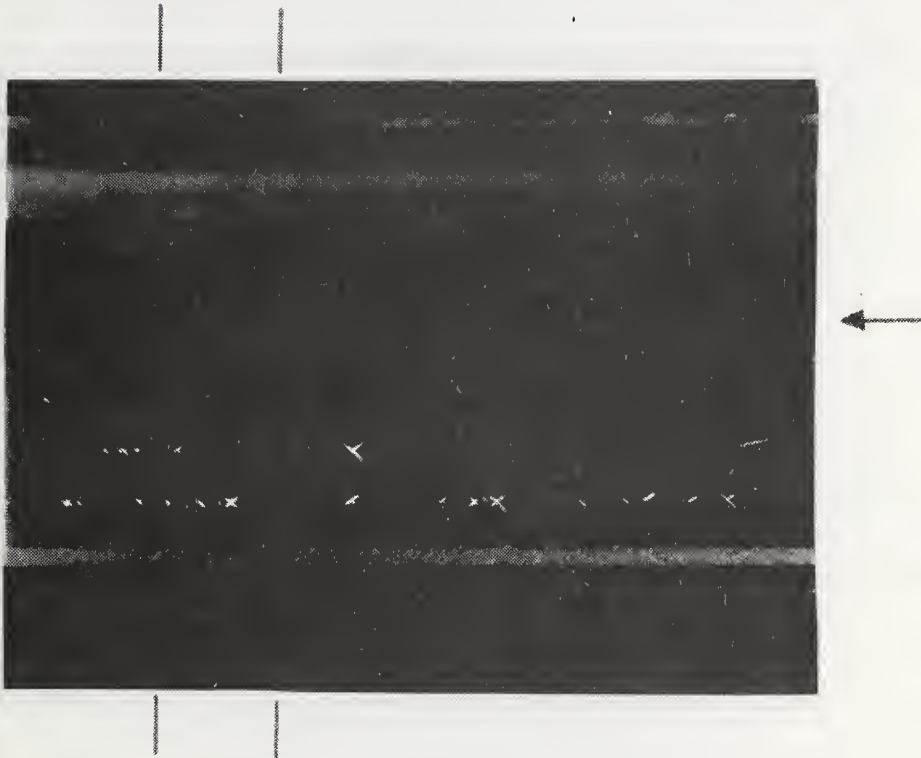


Fig. 2. Damage sites in calcite. These are the same sites as in Fig. 1 except they are viewed through a polarizer with side-light illumination. The same conventions are used as in Fig. 1. The magnification is 6.5X.

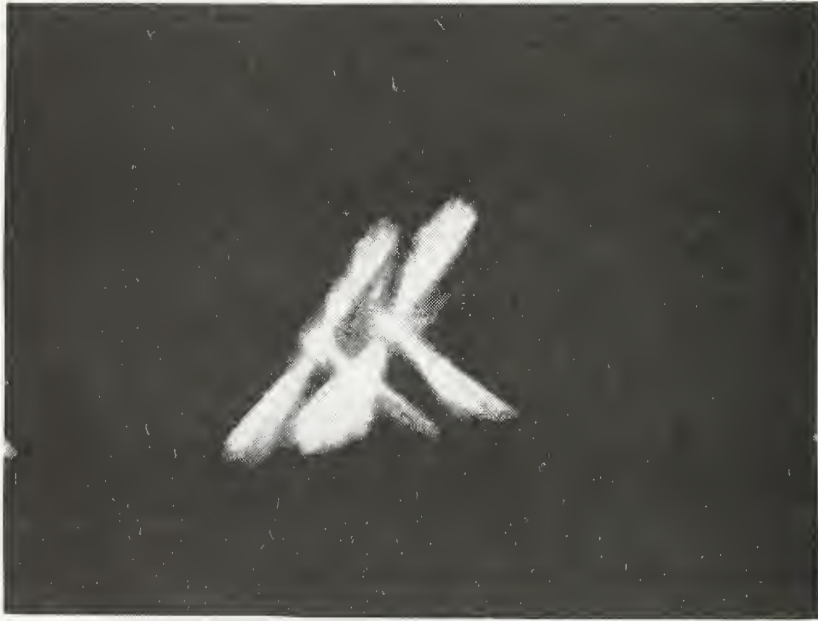


Fig. 3. Magnified view of a damage site in calcite as viewed with side-light illumination. The double image, which is due to the crystal birefringence, occurs because no polarizer was used for obtaining the photograph.

eliminate double image formation caused by the crystal birefringence. The arrows to the side of the figures show the direction of laser beam propagation, which was perpendicular to the optic axis. Damage sites whose ordinates are above the arrows were produced with the extraordinary ray; those below the arrows were produced with the ordinary ray. The vertical lines on the figures define the planes of focus; the left line defines for the ordinary ray focus, the right line defines the extraordinary ray focus.

Observe that the damage sites are randomly distributed about the focal planes. Filamentary damage, which is associated with self-focusing, is not seen. These observations are indicative of inclusion damage. In figure 3 we show a magnified view of one damage site. No polarizer was used in obtaining the photograph so that a double image appears due to the crystal birefringence. The damage has the appearance of feather-like cracks radiating from a central region which is the probable location of the inclusion. Setting a damage threshold for inclusion damage is difficult because the threshold will depend upon the diameter of the inclusion. Theoretical calculations [14,15] predict that, for our experimental parameters, spherical inclusions $\sim 0.2 \mu\text{m}$ will produce the lowest damage threshold.

Figures 4 to 7 are photographs of damage sites in KDP and KD*P. The arrows show the direction of the laser beam propagation, which was along the c-axis of the crystals. The vertical lines define the focal plane of the laser beam. The random distribution of the damage sites about the focal plane and the lack of filamentary damage

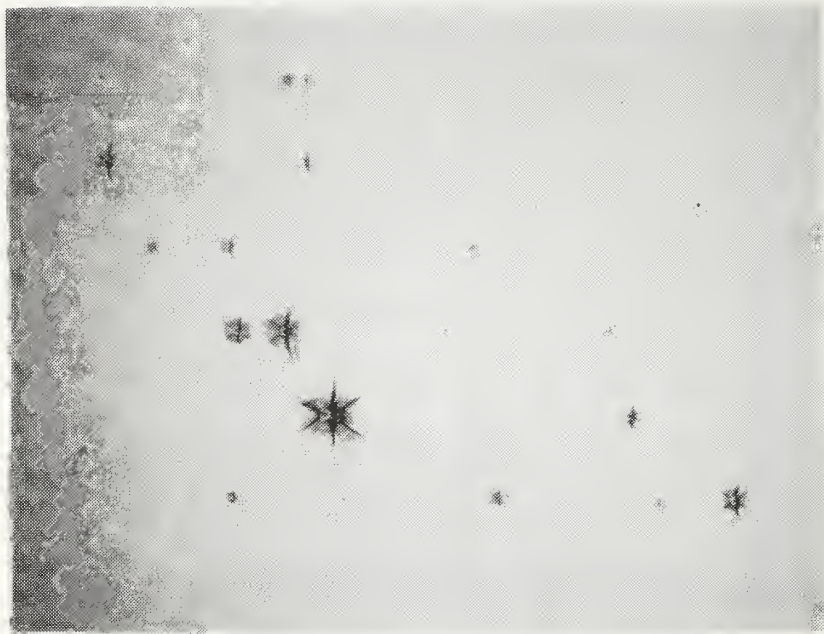


Fig. 4. Damage sites in KDP as viewed in transmitted white light. The vertical lines define the plane of focus. The arrow shows the direction of the laser beam propagation, which was along the crystallographic c-axis. The magnification is 7X.

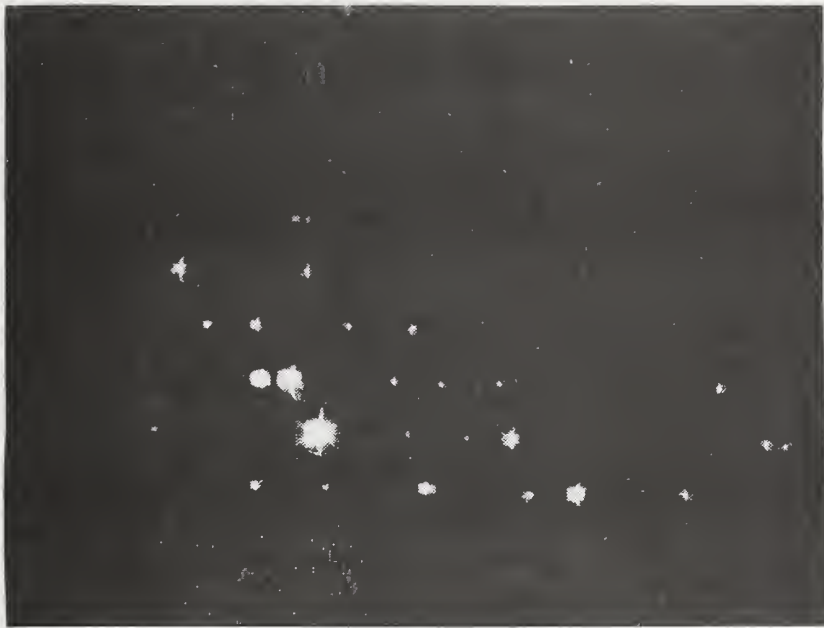


Fig. 5. Damage sites in KDP. These are the same sites as in Fig. 4 except they are viewed with side-light illumination. The conventions used are the same as in Fig. 4. The magnification is 4.5X.



Fig. 6. Damage sites in KD*P as viewed in transmitted white light. The conventions used are the same as in Fig. 4. The magnification is 7.5X.



Fig. 7. Damage sites in KD*P. These are the same sites as in Fig. 6 except they are viewed with side-light illumination. The conventions used are the same as in Fig. 4.

indicate that we are observing inclusion type damage. The morphology of the damage sites in KDP and KD*P is similar, but the sites have a different appearance than in calcite. The difference can most probably be attributed to the crystal structures of the materials.

Figures 8 and 9 are photographs of damage observed in LiNbO_3 . The arrows indicate the laser beam propagation direction, which was along the c-axis of the crystal. The vertical lines denote the focal plane of the laser beam. In figure 8 we can clearly observe damage caused by four laser shots. The uppermost series of damage sites (co-linear with the arrow) was produced by an 11.2 mJ pulse with a peak power of 380 KW. A filamentary damage track was produced, which is evidence for self-focusing. The filament is clearly seen in an enlargement which is shown in figure 10. In addition to observing self-focusing, in figure 9 we can also observe damage due to inclusions upstream from the filament. The three sets of damage sites below the large track of damage were all produced with pulses of the same energy (3.0 mJ). While the main damage occurs in the vicinity of the focal plane, it is clear that the damage process is non-reproducible. In glasses, we have observed that the damage process is reproducible. In figure 9 we can clearly observe damage sites far upstream from the focal plane. We conclude therefore that the main bulk damage mechanism in LiNbO_3 is due to inclusions. While it is possible to produce self-focusing damage, it is difficult to draw any conclusions about the self-focusing threshold and nonlinear index because the occulting effect of inclusions obscures the determination of the power involved in the self-focusing process.



Fig. 8. Damage sites in LiNbO_3 as viewed in transmitted white light. The conventions used are the same as in Fig. 4. The magnification is 6.5X. The damage opposite the arrow is indicative of self-focusing (see Fig. 10).



Fig. 9. Damage sites in LiNbO_3 . These are the same sites as in Fig. 8 except they are viewed with side-light illumination. The conventions used are the same as in Fig. 4. The magnification is 6X.



Fig. 10. Filamentary damage in LiNbO_3 which is indicative of self-focusing. The magnification is 42X.

In Table I we present an estimate of energy densities and maximum power densities of the laser beam in the vicinity of several damage sites in the crystals under study. We say vicinity because the numbers are calculated on the beam axis whereas the damage site may be off the axis. The values cannot be interpreted as thresholds but can be interpreted as upper bounds to thresholds. The sites chosen were the farthest upstream. We avoided sites near the focal plane because this is where aberrations are strongest. The energy and power densities are calculated from equations that define the propagation characteristics of Gaussian beams.

An examination of the table shows a large variation of energy density near damage sites in all the materials except calcite. In calcite the values appear to be quite reproducible even though they were obtained with laser shots of widely varying energy. The result suggests that the inclusions in calcite are of uniform size. An examination of the calcite crystal under illumination by a 5 mW helium-neon laser shows planes with a high density of scatterers. Many of the damage sites in calcite are located within these planes.

2.2. Self-Focusing in Yttrium Aluminum Garnet (YAG)

In our previous report we discussed measurements of filamentary damage tracks produced in YAG with linearly and circularly polarized radiation. The laser beam propagated along the [111] crystallographic axis. We found that the self-focusing lengths deduced from these measurements were in good agreement with theory [10,12,16].

Table I. Energy density and peak power density of laser beam in the vicinity of damage sites.

		Energy (mJ)	Energy Density (J/cm ²)	Power Density (W/cm ²)
Calcite	1	2.4	45	1.55×10^9
	2	14.4	46	1.56×10^9
	3	4.4	46	1.58×10^9
KDP	1	11.8	76	2.6×10^9
	2	13	130	4.5×10^9
	3	10.3	200	7.0×10^9
	4	24.2	460	15.7×10^9
KD*P	1	12.7	120	4.2×10^9
	2	12.7	280	9.5×10^9
	3	12.7	390	13.4×10^9
LiNbO ₃	1	3.03	24.2	0.71×10^9
	2	3.03	31.3	0.91×10^9
	3	11.2	72.2	2.5×10^9

In this report we present corrected values for the self-focusing thresholds deduced from the data. These corrections are due to a recalibration of our thermopile energy meter and to our taking into account reflections from our sample entrance face. The corrected thresholds for linearly and circularly polarized radiation are $P_c = 0.40$ MW and $P'_c = 0.50$ MW, respectively. (Throughout this section primed symbols refer to circular polarization; unprimed symbols refer to linear polarization.) In the theory of Dawes and Marburger, P_2 is the power above which the laser intensity diverges on the beam axis. Hence, damage will occur at powers less than P_2 . Thus $P_c < P_2$ because P_c is a measure of the damage threshold for the particular experimental conditions discussed in our previous report. We are actually measuring a damage threshold.

We have previously discussed a method of calculating the nonlinear index n_2 and the contributions that the Kerr, electrostrictive, and thermal effects might make to n_2 [10-12]. Here n_2 is defined by

$$\delta n_m = n_2 E_o^2 \quad (1)$$

where δn_m is the maximum refractive index change occurring during the passage of a laser pulse and E_o is the RMS value of the electric field at the peak of the pulse. In the paraxial ray approximation, the peak power of a pulse that leads to critical self-focusing of beams with a Gaussian profile, in which the spreading of the beam by diffraction is exactly cancelled by self-focusing, is given by [17-19]

$$P_c = \lambda^2 c / (32\pi^2 n_2) \quad (2)$$

where λ is the wavelength of the laser radiation in air, c is the

velocity of light, and $P_c = .273 P_2$ [16]. A lower bound for n_2 can be derived with eq (2); we obtain $n_2 = 2.7 \times 10^{-13}$ esu and $n_2' = 2.1 \times 10^{-13}$ esu. The contribution of electrostriction to n_2 is expected to be negligible because YAG has exceedingly small stress-optic coefficients. For a beam propagating along the [111] axis, the contributions of the Kerr effect to n_2 and n_2' have the relation $n_2(K)/n_2'(K) = 1.5$ if we assume that the Kerr effect is of electronic origin [20]. Using eqs (20a) and (20b) of reference [10], we find that $n_2(K) = 1.7 \times 10^{-13}$ esu and the thermal contribution $n_2(T) = 0.8 \times 10^{-13}$ esu. Thus we find that the Kerr effect is the dominant self-focusing mechanism. From $n_2(T)$ we calculate an absorption coefficient $\alpha = 5 \times 10^{-3} \text{ cm}^{-1}$ which is of the proper magnitude for YAG.

2.3. Damage in Neodymium-Doped Thorium:Yttrium Oxide Ceramic Laser Rod

In cooperation with Charles Greskovich of the General Electric Company Corporate Research and Development Center, we conducted damage studies in a laser rod constructed of neodymium-doped thorium:yttrium oxide ceramic material. A bulk damage threshold was obtained by focusing the laser beam into the sample. The damage threshold relative to several optical materials is given in Table II. Effects due to self-focusing may be present in the data. Figure 11 is a picture of a bulk damage site as viewed along the rod axis in transmitted white light. Note radial cracks that propagate with jogs caused probably by grain

Table II. Relative bulk damage thresholds in several materials and surface damage threshold of neodymium-doped thoria:yttrium oxide ceramic^a (yttralux)^b.

	Pulse Energy (mJ)	Peak Pulse Power (MW)
BSC 517	22	0.75
Dense Flint SF 55	3.74	0.128
Fused Silica	29	1.01
YAG	11	0.36
Yttralox (Bulk)	5.5	0.19
Yttralox (Surface)	1.5	0.051

^aObtained by focusing of the output of a Nd:glass laser (pulsewidth $\tau = 25$ ns) into the sample or on the surface of the sample with a 181-mm focal length lens.

^bCommercial materials are identified in this report to specify the particular substance on which the data were obtained. In no instance does such identification imply recommendation or endorsement by the National Bureau of Standards or that the material identified is necessarily the best for any application.



Fig. 11. Bulk damage site in a laser rod of neodymium-doped thoria:yttrium oxide ceramic as viewed along the rod axis in transmitted white light. The magnification is 75X. Note radial cracks that propagate with jogs caused probably by grain boundaries.



Fig. 12. The same damage site as in Fig. 11 but viewed between crossed polarizers. Note the highly strained region in the immediate vicinity of the damage site and also note the revelation of grain boundaries under stress. The magnification is 75X.

boundaries. Figure 12 is a picture of the same bulk damage site as viewed between crossed polarizers. Note the highly strained region in the immediate vicinity of the damage site and note also the grain boundaries revealed by the stress. The average diameter of the strain field is approximately 1.5 mm.

In addition to bulk damage, we produced surface damage on the laser rod by focusing the laser beam onto the sample surface. Figure 13 is a reflected light micrograph of a surface damage site located at a three-grain intersection. There is a fine network of micro-cracks in one grain. All three grains had originally exhibited this appearance, but, in the process of cleaning the surface for picture taking, material flaked off the other two grains. Note that the general surface condition is characterized by polishing scratches.

2.4. Relations Between Electrostriction and the Stress-Optic Effect

The process of electrostriction is of current interest because it can cause the self-focusing of high-intensity radiation in solids. Articles have been published that relate the electrostrictive coefficients to the stress-optic [21], elasto-optic [22], or piezodielectric coefficients [23] with differing results. In an early work, Guggenheim [24] has derived similar relations for liquids which undergo magnetostriction. He showed that the particular relationship obtained will depend upon the boundary conditions much as the electric polarization in a solid depends upon the shape of the solid. Guggenheim showed that solutions are easily obtained only for relatively simple

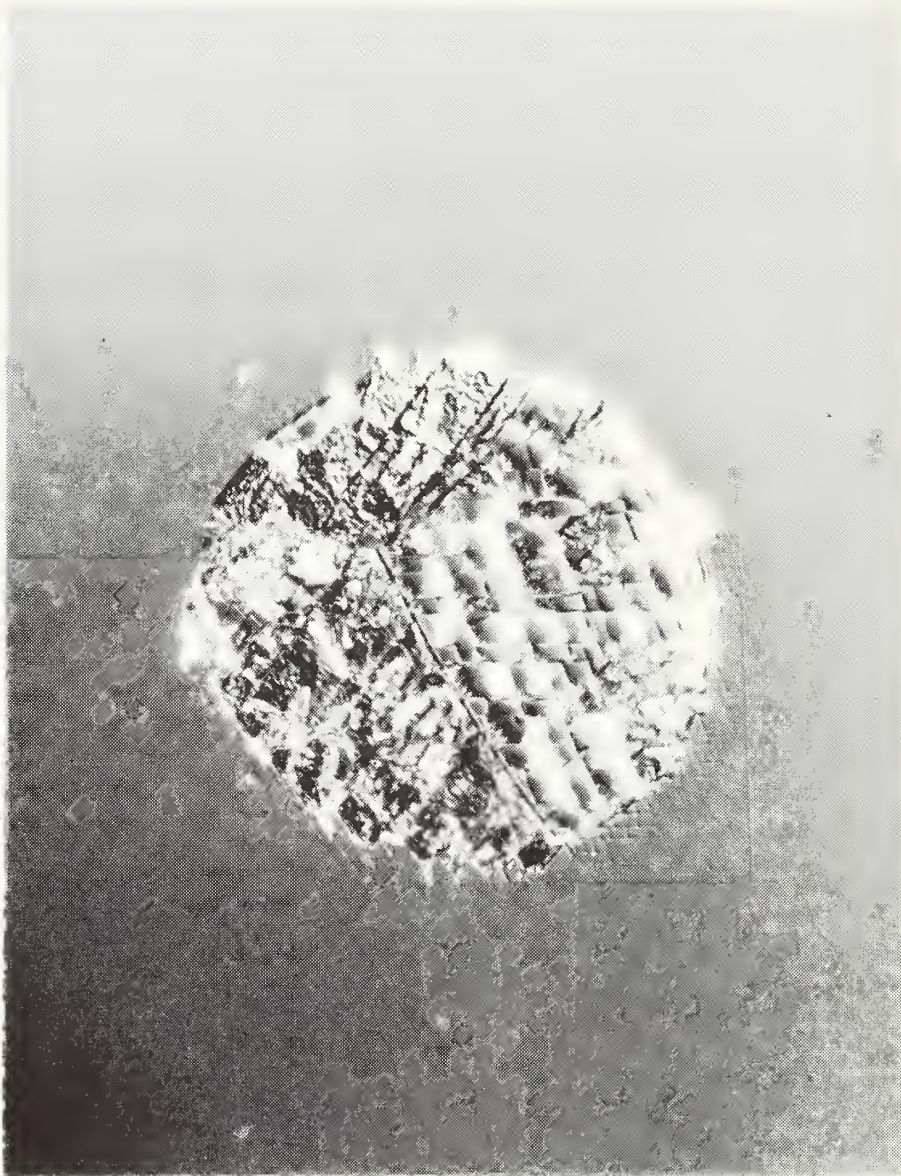


Fig. 13. Damage site on the surface of thoria:yttrium oxide ceramic laser rod. This picture is a reflected-light micrograph of a surface damage site located at a three-grain intersection. The magnification is 750X.

configurations.

In this report we derive relations between the electrostrictive coefficients and the stress-optic coefficients for dielectric materials with inversion symmetry, based on Guggenheim's work. We ignore any effects due to body rotations. Three cases are treated. The following notation is used: V_E is the volume occupied by the electric field; V_S is the volume of the solid in the absence of strain; κ_{ij} is an element of the dielectric tensor and κ_{ij}^{-1} is an element of its inverse tensor; ϵ_{ij} is an element of the strain tensor; σ_{ij} is an element of the mechanical stress tensor; q_{ijkl} is a stress-optic coefficient; p_{ijkl} is an elasto-optic coefficient; and γ_{ijkl} is an electrostriction coefficient; s_{ijkl} is an elastic compliance coefficient. The phenomenological relationships among these constants are

$$D_i = \kappa_{ij} E_j; E_i = \kappa_{ij}^{-1} D_j \quad (1)$$

$$\Delta \kappa_{ij}^{-1} = q_{ijkl} \sigma_{kl} = p_{ijkl} \epsilon_{kl} \quad (2)$$

$$\epsilon_{kl} = \frac{1}{2} \gamma_{ijkl} E_i E_j + s_{klmn} \sigma_{mn} \quad (3)$$

In eq (2) we ignore the term quadratic in electric field, the Kerr effect term. Equations (1) and (2) are taken to apply when the fields are either constant or time varying and stresses and strains are constant in time. When the fields are time varying, we take a time average of $E_i E_j$ in eq (3). The tensors κ , κ^{-1} , q , p and γ will depend upon the frequency of the field.

Following Guggenheim, we can write the free energy of a system in any one of the following forms, depending on which variables are meant to be independent:

$$F_1 = U - TS - \frac{1}{4\pi} \int E_i D_i \, dV - \int \sigma_{ij} \epsilon_{ij} \, dV \quad (4a)$$

$$F_2 = U - TS - \int \sigma_{ij} \epsilon_{ij} \, dV \quad (4b)$$

$$F_3 = U - TS - \frac{1}{4\pi} \int E_i D_i \, dV \quad (4c)$$

$$F_4 = U - TS \quad (4d)$$

We integrate over a fixed volume of space, which includes V_E and V_S .

U is the internal energy; T is the temperature; S is the entropy. The change in internal energy of the system is given by [25]

$$\delta U = T \delta S + \frac{1}{4\pi} \int E_i \delta D_i \, dV + \int \sigma_{ij} \delta \epsilon_{ij} \, dV \quad (S, D, \epsilon)$$

where the independent variables are listed to the right. The same convention is followed below. We then obtain

$$\delta F_1 = -S \delta T - \frac{1}{4\pi} \int D_i \delta E_i \, dV - \int \epsilon_{ij} \delta \sigma_{ij} \, dV \quad (T, E, \sigma) \quad (5a)$$

$$\delta F_2 = -S \delta T + \frac{1}{4\pi} \int E_i \delta D_i \, dV - \int \epsilon_{ij} \delta \sigma_{ij} \, dV \quad (T, D, \sigma) \quad (5b)$$

$$\delta F_3 = -S \delta T - \frac{1}{4\pi} \int D_i \delta E_i \, dV + \int \sigma_{ij} \delta \epsilon_{ij} \, dV \quad (T, E, \epsilon) \quad (5c)$$

$$\delta F_4 = -S \delta T + \frac{1}{4\pi} \int E_i \delta D_i \, dV + \int \sigma_{ij} \delta \epsilon_{ij} \, dV \quad (T, D, \epsilon) \quad (5d)$$

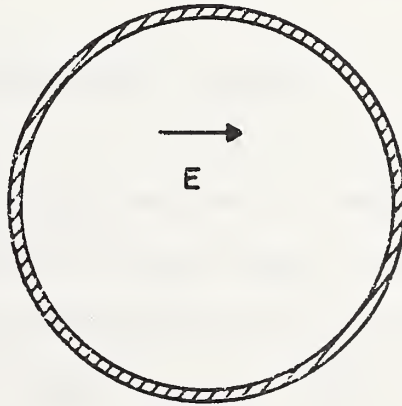
Similar expressions can be derived with S as an independent variable. The above expressions will be used to obtain the desired relationships between γ , q , and κ .

2.4.1. Case I

We have a solid of volume V_S . A uniform electric field is totally enclosed within V_S except for in a thin layer of material at the boundary of the solid in which the field falls to zero. When the solid undergoes a strain, we assume that the electric field is still enclosed within the solid, but V_E is unchanged. We choose this geometry in order to neglect the stresses developed because of the constraining effect of the field free region of the solid. For sufficiently large volumes, V_S can be considered equal to V_E . Using eq (5a), we obtain

$$\delta F_1 = - SdT - \frac{V_E}{4\pi} \kappa_{ij} E_i dE_j - V_S \epsilon_{ij} d\sigma_{ij} \quad (6)$$

CASE I



For an isothermal process

$$\kappa_{ij} = - \left[\frac{4\pi}{V_S} \frac{\partial^2 F_1}{\partial E_i \partial E_j} \right]_{T, \sigma} \quad (7)$$

and

$$\epsilon_{ij} = - \left[\frac{1}{V_S} \frac{\partial F_1}{\partial \sigma_{ij}} \right]_{T, E} \quad (8)$$

Taking higher derivatives, we obtain

$$\frac{1}{4\pi} \frac{\partial \kappa_{ij}}{\partial \sigma_{kl}} = \frac{\partial^2 \epsilon_{kl}}{\partial E_i \partial E_j} \quad (9a)$$

Using eq (5b), we obtain a similar result

$$\frac{1}{4\pi} \frac{\partial \kappa_{ij}^{-1}}{\partial \sigma_{kl}} = - \frac{\partial^2 \epsilon_{kl}}{\partial D_i \partial D_j} \quad (9b)$$

Equations (9a) and (9b) lead to the equality

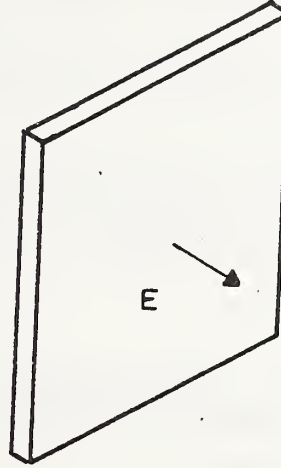
$$\gamma_{ijkl} = - \frac{1}{4\pi} \kappa_{im} \kappa_{jn} q_{mnkl} \quad (10)$$

Equation (10) is used for calculating the electrostrictive strains induced by focusing a laser beam into the interior of a solid. It corresponds to the results of references [19] and [21].

2.4.2. Case II

Consider a thin slab of material in an external E field with the large faces of the slab perpendicular to the field.

CASE II



In this case it is convenient to use eq (5b) because D is continuous across the slab boundary. End effects are neglected. We obtain

$$\delta F_2 = - SdT + \frac{V_E}{4\pi} D_i dD_i + (\kappa_{ij}^{-1} - \delta_{ij})(1 + \epsilon_{mn} \delta_{mn}) V_S D_i dD_j - V_S \epsilon_{ij} d\sigma_{ij} \quad (11)$$

Taking derivatives for the isothermal case, we obtain

$$\left[\frac{1}{V_S} \frac{\partial F_2}{\partial \sigma_{kl}} \right]_{T,D} = - \epsilon_{kl} \quad (12)$$

$$\left[\frac{\partial^2 F_2}{\partial D_i \partial D_j} \right]_{T,\sigma} = \frac{V_S}{4\pi} (\kappa_{ij}^{-1} - \delta_{ij})(1 + \epsilon_{mn} \delta_{mn}) + \frac{V_E}{4\pi} \delta_{ij} \quad (13)$$

Taking higher order derivatives and keeping terms to lowest order, we obtain

$$\frac{\partial^2 \epsilon_{kl}}{\partial D_i \partial D_j} = -\frac{1}{4\pi} \frac{\partial \kappa_{ij}^{-1}}{\partial \sigma_{kl}} - \frac{1}{4\pi} (\kappa_{ij}^{-1} - \delta_{ij}) \delta_{mn} s_{mnkl} \quad (14)$$

or

$$\gamma_{pqkl} = -\frac{1}{4\pi} \kappa_{pi} \kappa_{qj} \left[q_{ijkl} + (\kappa_{ij}^{-1} - \delta_{ij}) \delta_{mn} s_{mnkl} \right] \quad (15)$$

2.4.3. Case III

Consider a long narrow cylinder whose axis lines up parallel to a uniform electric field.



In this case it is convenient to use eq (5a) because E is continuous across the cylinder wall. End effects are neglected. We obtain

$$\delta F_1 = -SdT - \frac{V_E}{4\pi} E_i dE_i - (\kappa_{ij} - \delta_{ij}) (1 + \epsilon_{mn} \delta_{mn}) V_S E_i dE_j - V_S \epsilon_{ij} d\sigma_{ij} \quad (16)$$

Taking derivatives for the isothermal case, we obtain

$$\left. \frac{1}{V_S} \frac{\partial F_1}{\partial \sigma_{kl}} \right|_{T,E} = - \epsilon_{kl} \quad (17)$$

$$\left. \frac{\partial F_1}{\partial E_i \partial E_j} \right|_{T,\sigma} = - \frac{V_E}{4\pi} \delta_{ij} - \frac{V_S}{4\pi} (\kappa_{ij} - \delta_{ij}) (1 + \epsilon_{mn} \delta_{mn}) \quad (18)$$

Taking higher order derivatives and keeping terms to lowest order, we obtain

$$\frac{\partial^2 \epsilon_{kl}}{\partial E_i \partial E_j} = \frac{1}{4\pi} \frac{\partial \kappa_{ij}}{\partial \sigma_{kl}} + \frac{1}{4\pi} (\kappa_{ij} - \delta_{ij}) \delta_{mn} s_{mnkl} . \quad (19)$$

But, the susceptibility is

$$\chi_{ij} = \frac{\kappa_{ij} - \delta_{ij}}{4\pi} \quad (20)$$

so that

$$\gamma_{ijkl} = - \frac{1}{4\pi} \kappa_{im} \kappa_{jn} s_{mnkl} + \chi_{ij} \delta_{mn} s_{mnkl} . \quad (21)$$

Equation (21) corresponds to the results of Maradudin and Burstein [22].

2.5 Acknowledgments

We would like to thank Alvin Rasmussen and Dale West of the National Bureau of Standards for the calibration of our thermopile.

The photographs and descriptions of the damage sites in the neodymium-doped thoria:yttrium oxide ceramic laser rod (figures 11-13) were supplied by Charles Greskovich.

2.6. References

- [1] A. A. Poplavskii and L. D. Khazov, "Anisotropic Resistance of CaCO_3 to Laser Radiation," Zh. Tekh. Fiz. 2, 407 (1969) [Sov. Phys.--Tech. Phys.].
- [2] G. M. Zverev, E. A. Levchuk, and E. K. Maldutis, "Destruction of KDP, ADP, and LiNbO_3 Crystals by Intense Laser Radiation," Zh. Eksp. Teor. Fiz. 57, 730 (1969) [Sov. Phys.--JETP 30, 400 (1970)].
- [3] Michael Bass, "Nd:YAG Laser Irradiation Induced Damage to LiNbO_3 and KDP," IEEE J. Quantum Electron. QE-7, 350 (1971).
- [4] G. M. Zverev, E. A. Levchuk, V. A. Paskov and Yu. D. Poyadin, "Damage to the Surface of Lithium Niobate by Light," Zh. Eksp. Teor. Fiz. 62, 307 (1972) [Sov. Phys.--JETP 35, 165 (1972)].
- [5] W. D. Fountain, L. M. Osterink, and G. A. Massey, in Damage in Laser Materials: 1971, NBS Special Publication 356 (U.S. Government Printing Office, Washington, D. C., 1971), p. 91.
- [6] W. A. Massey and W. R. Hook, "Lithium Niobate Damage Threshold Measurements Inside a Nd:YAG Q-Switched Laser Cavity," IEEE J. Quantum Electron. QE-7, 317 (1971).
- [7] M. Bass and H. H. Barrett, in Laser Induced Damage in Optical Materials: 1972, NBS Special Publication 372 (U. S. Government Printing Office, Washington, D. C., 1972), p. 58.
- [8] M. Bass and H. H. Barrett, in Damage in Laser Materials: 1971, NBS Special Publication 356 (U. S. Government Printing Office, Washington, D. C., 1971), p. 76.

- [9] Michael Bass, in Damage in Laser Materials, NBS Special Publication 341 (U. S. Government Printing Office, Washington, D. C., 1970), p. 90.
- [10] A. Feldman, D. Horowitz, and R. M. Waxler, "Laser Damage in Materials," National Bureau of Standards Report NBSIR 73-119 (1973).
- [11] A. Feldman, D. Horowitz, and R. M. Waxler, "Mechanisms for Self-Focusing in Optical Glasses," IEEE J. Quantum Electron., to be published.
- [12] A. Feldman, D. Horowitz, and R. M. Waxler, in Damage in Laser Materials: 1973, NBS Special Publication, to be published.
- [13] N. Boling, in Damage in Laser Materials: 1973, NBS Special Publication, to be published.
- [14] H. S. Bennett, in Damage in Laser Materials, NBS Special Publication 341 (U. S. Government Printing Office, Washington, D. C., 1970), p. 51.
- [15] R. W. Hopper, C. Lee, and D. R. Uhlmann, in Damage in Laser Materials, NBS Special Publication 341 (U. S. Government Printing Office, Washington, D. C., 1970), p. 55.
- [16] E. L. Dawes and J. H. Marburger, "Computer Studies in Self-Focusing," Phys. Rev. 179, 862 (1969).
- [17] W. G. Wagner, H. A. Haus, and J. H. Marburger, "Large-Scale Self-Trapping of Optical Beams in the Paraxial Ray Approximation," Phys. Rev. 175, 256 (1968).
- [18] G. M. Zverev and V. A. Pashkov, "Self-Focusing of Laser Radiation in Solid Dielectrics," Zh. Eksp. Teor. Fiz. 57, 1128

- (1969) [Sov. Phys.--JETP 30, 616 (1970)].
- [19] E. L. Kerr, "Track Formation in Optical Glass Caused by Electrostrictive Laser Beam Self-Focusing," Phys. Rev. A 4, 1195 (1971).
- [20] P. D. Maker and R. W. Terhune, "Study of Optical Effects Due to an Induced Polarization Third Order in the Electric Field Strength," Phys. Rev. 137, A801 (1965).
- [21] A. A. Gundjian, "Electrostriction in Germanium," Solid State Commun. 3, 279 (1965).
- [22] A. A. Maradudin and E. Burstein, "Relation Between Photoelasticity, Electrostriction, and First Order Raman Effect in Crystals of the Diamond Structure," Phys. Rev. 164, 1081 (1967).
- [23] H. Osterberg and J. W. Cookson, "The Piezodielectric Effect and Electrostriction in Anisotropic or Isotropic Media," Phys. Rev. 51, 1096 (1937).
- [24] E. A. Guggenheim, "The Thermodynamics of Magnetization," Proc. Roy. Soc. (London) A, 155, 70 (1936).
- [25] E. A. Guggenheim, "On Magnetic and Electrostatic Energy," Proc. Roy. Soc. (London) A, 155, 49 (1936).

U.S. DEPT. OF COMM. BIBLIOGRAPHIC DATA SHEET	1. PUBLICATION OR REPORT NO. NBSIR 73-268	2. Gov't Accession No.	3. Recipient's Accession No.
4. TITLE AND SUBTITLE Laser Damage in Materials		5. Publication Date August 1973	
		6. Performing Organization Code NBSIR 73-268	
7. AUTHOR(S) Albert Feldman, Deane Horowitz, and Roy M. Waxler		8. Performing Organization	
9. PERFORMING ORGANIZATION NAME AND ADDRESS NATIONAL BUREAU OF STANDARDS DEPARTMENT OF COMMERCE WASHINGTON, D.C. 20234		10. Project/Task/Work Unit No. 3130440	
		11. Contract/Grant No. 2016/3D10	
12. Sponsoring Organization Name and Address Advanced Research Projects Agency Arlington, Virginia 22209		13. Type of Report & Period Covered Semi-Annual Tech. 2-1-73 to 7-31-73	
		14. Sponsoring Agency Code	
15. SUPPLEMENTARY NOTES			
16. ABSTRACT (A 200-word or less factual summary of most significant information. If document includes a significant bibliography or literature survey, mention it here.) Neodymium:glass laser induced damage is observed in lithium niobate (LiNbO_3), calcite (CaCO_3), potassium dihydrogen phosphate (KDP), and deuterated potassium dihydrogen phosphate (KD^*P). The damage at the lowest power levels is caused by inclusions. At higher power levels, filamentary damage, which is indicative of self-focusing, is observed in LiNbO_3 . An analysis of self-focusing data in yttrium aluminum garnet shows that the Kerr effect is the dominant self-focusing mechanism, with some contribution from the thermal effect. Bulk and surface damage thresholds in neodymium-doped thoria:yttrium oxide ceramic are obtained relative to bulk damage thresholds in several optical materials. For solid materials relationships are obtained between the stress-optic coefficients and the electrostrictive coefficients under different geometric boundary conditions.			
17. KEY WORDS (Alphabetical order, separated by semicolons) Absorption coefficient; calcite; damage threshold; deuterated potassium dihydrogen phosphate; electrostriction; electrostrictive self-focusing; inclusion damage; Kerr effect; laser damage; lithium niobate; nonlinear index of refraction; potassium dihydrogen phosphate; self-focusing; thermal self-focusing; thoria:yttrium oxide ceramic; yttrium aluminum garnet.			
18. AVAILABILITY STATEMENT <input checked="" type="checkbox"/> UNLIMITED. <input type="checkbox"/> FOR OFFICIAL DISTRIBUTION. DO NOT RELEASE TO NTIS.		19. SECURITY CLASS (THIS REPORT) UNCLASSIFIED	21. NO. OF PAGES 39
		20. SECURITY CLASS (THIS PAGE) UNCLASSIFIED	22. Price



